

## Magnetic Moment Preservation and Emergent Kondo Resonance of Co-Phthalocyanine on Semimetallic Sb(111)

Limin She<sup>1,\*</sup>, Zhitao Shen<sup>1,\*</sup>, Zhenyang Xie<sup>1</sup>, Limei Wang<sup>1</sup>, Yeheng Song,<sup>1</sup>  
Xue-Sen Wang,<sup>2,1</sup> Yu Jia,<sup>1,3,4</sup> Zhenyu Zhang,<sup>5,†</sup> and Weifeng Zhang<sup>1,‡</sup>

<sup>1</sup>Key Laboratory for Quantum Matters, and Key Laboratory of Photovoltaic Materials, Henan University, Kaifeng 475004, China

<sup>2</sup>Department of Physics, National University of Singapore, 117542, Singapore

<sup>3</sup>International Laboratory for Quantum Functional Materials of Henan, Zhengzhou University, Zhengzhou 450003, China

<sup>4</sup>Key Laboratory for Special Functional Materials of Ministry of Education, Henan University, Kaifeng 475004, China

<sup>5</sup>International Center for Quantum Design of Functional Materials (ICQD), University of Science and Technology of China, Hefei 230026, China

 (Received 17 September 2021; revised 28 March 2022; accepted 25 May 2022; published 6 July 2022)

Magnetic molecules on surfaces have been widely investigated to reveal delicate interfacial couplings and for potential technological applications. In these endeavors, one prevailing challenge is how to preserve or recover the molecular spins, especially on highly metallic substrates that can readily quench the magnetic moments of the admolecules. Here, we use scanning tunneling microscopy and spectroscopy to exploit the semimetallic nature of antimony and observe, surprisingly yet pleasantly, that the spin of Co-phthalocyanine is well preserved on Sb(111), as unambiguously evidenced by the emergent strong Kondo resonance across the molecule. Our first-principles calculations further confirm that the optimal density of states near the Fermi level of the semimetal is a decisive factor, weakening the overall interfacial coupling, while still ensuring sufficiently effective electron-spin scattering in the many-body system. Beyond isolated admolecules, we discover that each of the magnetic moments in a molecular dimer or a densely packed island is distinctly preserved as well, rendering such molecular magnets immense potentials for ultrahigh density memory devices.

DOI: [10.1103/PhysRevLett.129.026802](https://doi.org/10.1103/PhysRevLett.129.026802)

Molecular magnets are appealing elemental building blocks for realizing nanoscale information storage and spintronic devices [1–6]. When adsorbed, their electronic and magnetic properties can be substantially modified by the hosting substrates, with the underlying nature of interfacial couplings sensitively dependent on the specific molecule-substrate combinations [7–21]. For a given system, a comprehensive understanding of the fundamental interfacial processes is a prerequisite in gaining precise control of the magnetic properties of the admolecule for desirable functionalities.

In the endeavor of exploiting admolecule based spintronic devices, a widely studied species is Co-phthalocyanine (CoPc), with spin 1/2. However, the intrinsic magnetic moment of CoPc is quenched when adsorbed on highly metallic substrates such as Cu(111), Ag(111), Au(111), and even on ferromagnetic Fe(110), and the underlying reason is mainly attributed to pronounced net charge transfer or strong interfacial bonding [7,17,18,22–24]. To date, various ingenious approaches, including bond-selective dehydrogenation and insertion of a buffer layer, have been devised to recover the magnetic moment of the adsorbed CoPc [7,18,25]. Theoretical studies have also revealed that the interfacial hybridization strengths can strongly affect the magnetic properties of CoPc, and can be substantially tuned by

changing the molecule-substrate separation for a given system [17,26]. Beyond such prevailing interface modification schemes, it is even more attractive to identify substrates that can naturally preserve the intrinsic moment of CoPc while also embodying rich many-body physics of electron-spin interfacial coupling to be elucidated.

In this Letter, we combine experimental and theoretical approaches to establish the vital role of an optimal density of states around the Fermi level of the substrate in preserving the intrinsic spin of the adsorbed CoPc molecule. Using scanning tunneling microscopy and spectroscopy (STM and STS), we find, surprisingly and yet pleasantly, a CoPc molecule on the semimetallic Sb(111) substrate exhibits spatially extended Kondo resonance even at the relatively high temperature of  $\sim 200$  K, an unambiguous indication that its molecular spin is well preserved upon adsorption. Our first-principles calculations within density functional theory (DFT) further show that the interfacial hybridization is optimized, allowing the unpaired  $d_{z^2}$  orbital of CoPc to endure the adsorption and interfacial charge transfer while also ensuring sufficiently effective spin-flip scattering of the many-body electrons of the semimetallic Sb(111). Moreover, the DFT calculations reveal that the interfacial charge transfer induces intramolecular reorganization of the spin density.

Beyond isolated molecules, our STS measurements further resolve that each of the CoPc molecules in a closely coupled molecular dimer or a densely packed molecular island distinctly exhibits its own Kondo resonance even in the likely presence of antiferromagnetic intermolecular RKKY coupling. Therefore, the CoPc assembly may serve as a platform for ultrahigh-density spin devices.

The experiments were carried out by using two commercial STM (Unisoku and Omicron) with a base pressure better than  $1.0 \times 10^{-10}$  Torr [see Sec. I in Supplemental Material (SM) [27]]. Figure 1(a) shows a high resolution STM image of three isolated CoPc molecules adsorbed at the bridge sites of Sb(111), exhibiting nearly flat-lying adsorption configurations. At a refined level, there exist two orientations of the admolecules,  $S_1$ , where the molecular lobes point to the  $[\bar{2}11]$  and  $[01\bar{1}]$  directions, and  $S_2$ , rotated by  $\sim 30^\circ$  from  $S_1$ . These configurations are consistent with previous identifications [35]. To understand their electronic properties, differential conductance spectra ( $dI/dV$ ) were taken at the Co ions of both configurations at 5 K. As shown in Fig. 1(b), the narrow peaks in the  $dI/dV$  spectra are located at  $\sim 10$  and 3 meV below  $E_F$  for  $S_1$  and  $S_2$ , respectively. Here, we note that, since the peaks

associated with the CoPc- $d_{z^2}$  orbital-mediated tunneling are typically located about 0.1–0.4 eV below  $E_F$  with a width of  $\sim 100$  meV, the sharp peaks very close to  $E_F$  observed here must be due to different physical origin(s) [7,36].

As a natural interpretation, we attribute the above peaks near  $E_F$  to the Kondo resonances, originating from the multiple spin-flip scatterings of the conduction electrons at the intrinsic spins of the molecules. Such an interacting many-body system can be well described by the Fano model, and the line shape of the  $dI/dV$  spectra in Fig. 1(b) can be fitted by the Fano formula as [28,38–40],

$$\frac{dI}{dV} \propto \frac{(\varepsilon + q)^2}{1 + \varepsilon^2}, \quad \varepsilon = \frac{eV - \varepsilon_0}{\Gamma_{\text{fit}}},$$

where  $q$  is the asymmetric Fano factor,  $\varepsilon_0$  is the energy shift of the Kondo resonance center from  $E_F$ , and  $\Gamma_{\text{fit}}$  is half of the fitted width of the resonance. For the  $S_1$  and  $S_2$  configurations, after subtracting the contributions of the lock-in modulation [see Eq. (S5) in Supplemental Material [27]], we acquire the average values of the half-width of the resonance depending on experimental temperature to be  $\Gamma = 26.8 \pm 2$  and  $24.1 \pm 2$  meV, respectively. The Kondo

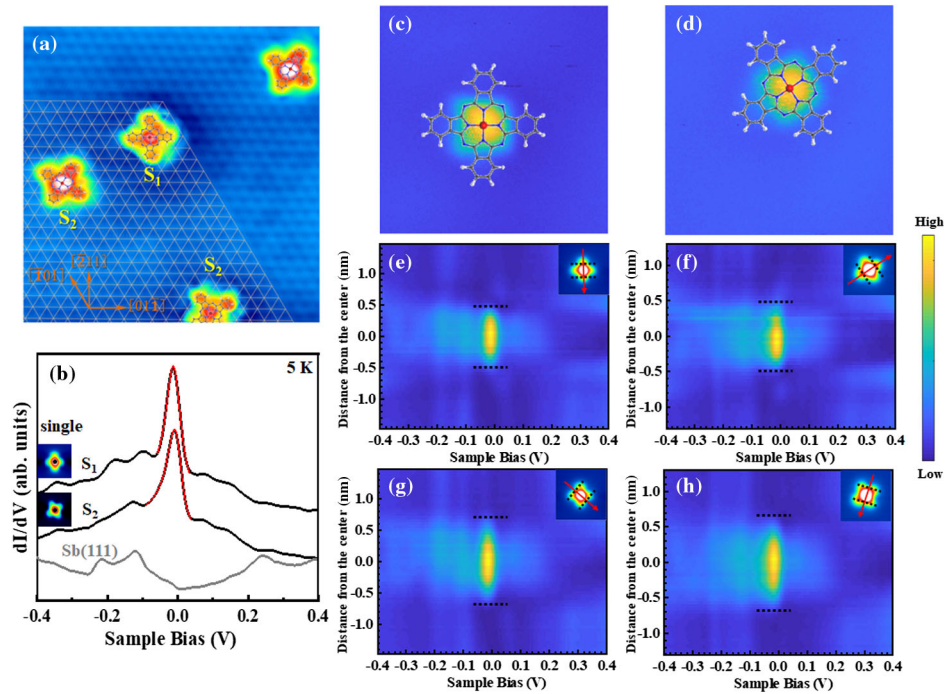


FIG. 1. (a) High resolution STM image ( $9.1 \times 9.1$  nm<sup>2</sup>;  $U = 0.4$  V;  $I = 300$  pA) with the isolated CoPc molecules and substrate lattice resolved simultaneously. The orange grid represents the substrate lattice, showing two configurations ( $S_1$  and  $S_2$ ), where the molecules are adsorbed at the bridge site of the substrate. The crystallographic directions of the Sb(111) substrate are denoted by the orange arrows. (b)  $dI/dV$  spectra for bare Sb(111) and the two configurations, acquired on the Co center of the isolated molecules on Sb (111) at 5 K. In the spectra (gray) from bare Sb(111), the three peaks at about  $-220$  mV,  $-120$  mV, and  $240$  mV correspond to the Dirac point and bending positions in the surface state bands, respectively [37]. (c) and (d)  $dI/dV$  mapping for both configurations, taken at  $-10$  and  $-3$  mV, respectively ( $4.0 \times 4.0$  nm<sup>2</sup>;  $I = 100$  pA). (e)–(h) Spatially dependent  $dI/dV$  spectra of the isolated CoPc molecules acquired along the lines marked by the red arrows in the insets. The black dashed lines roughly indicate the ranges of the Kondo resonance extending over the CoPc molecules.

temperatures are determined to be  $T_K = 219.7 \pm 17$  K ( $S_1$ ) and  $T_K = 197.3 \pm 17$  K ( $S_2$ ) according to the relationship  $\Gamma = \sqrt{2(k_B T_K)^2 + (\pi k_B T)^2}$ , where  $T$  is the substrate temperature, and  $k_B$  is the Boltzmann constant [28]. The observed  $T_K$  is very close to that of Co atoms on Sb(111) and dehydrogenated CoPc ( $d$ -CoPc) on Au(111) [7,37,41]. Here, it is worthwhile to note that Co atoms on Sb(111) can still exhibit Kondo resonance because such atoms possess spins of  $3/2$ , more robust against quenching due to charge transfer [42,43].

To reveal the spatial distribution of the Kondo resonance,  $dI/dV$  maps were acquired at sample voltages corresponding to the peak energy of the resonance, as shown in Figs. 1(c) and 1(d). Compared with the STM topographies [see Figs. S2(b) and S2(c) in SM [27]], we find that the Kondo resonance of CoPc is not only located at the Co ion, but also extends to the molecular pyrrole groups. This spatial distribution of the Kondo resonance is often driven by the  $\pi$ - $d$  interaction or the reorganization of the molecular charge density, which is further verified by a series of  $dI/dV$  spectra acquired along different axes over the CoPc molecule [8,20]. As shown in Figs. 1(e)–1(h), the Kondo resonance decays slowly as the STM tip moves away from the center of the molecule along two different directions. For a given configuration, the half-widths of the Kondo resonance are almost identical at Co and pyrrole ring [see Figs. S3(a) and S3(b) in SM [27]], indicating nearly uniform Kondo temperatures as well.

To gain deeper insight into the origin of the resonance peak near  $E_F$ , we have performed first-principles studies of the CoPc/Sb(111) system [see Sec. III in SM [27]]. In doing so, we construct the initial modes of CoPc molecules at the bridge sites of Sb(111) based on the STM results. Two stable adsorption configurations are identified, in which the CoPc molecules lie largely flat, but slightly concaved. Figures 2(a)–2(c) demonstrate the calculated spin-polarized partial densities of states (PDOS) on the Co ion and phthalocyanine (Pc) ligand in the free CoPc,  $S_1$ , and,  $S_2$  configurations, respectively, where the majority and minority spins of the  $d$  orbitals are clearly unevenly occupied. Especially, all the  $d_{z^2}$  orbitals are singly occupied, contributing significantly to the magnetic moment of the CoPc/Sb(111) composite. It is also noted that the  $d_{z^2}$  orbital near  $E_F$  in either configuration becomes broader when the molecule is adsorbed on Sb(111), indicating strong coupling between the discrete  $d_{z^2}$  spin state and surrounding conduction electron continuums of the Fano system.

In order to further unravel the nature of the interfacial coupling, we calculate the PDOS of bare Sb(111) and CoPc/Sb(111) complexes [Figs. 2(d)–2(f)]. We first note that the DOS of the complex near  $E_F$  is significantly lower than that of Cu(111), explaining why in the latter case the magnetic moment of CoPc is readily quenched [26], see Fig. S4 in SM [27]). For our present system, we propose

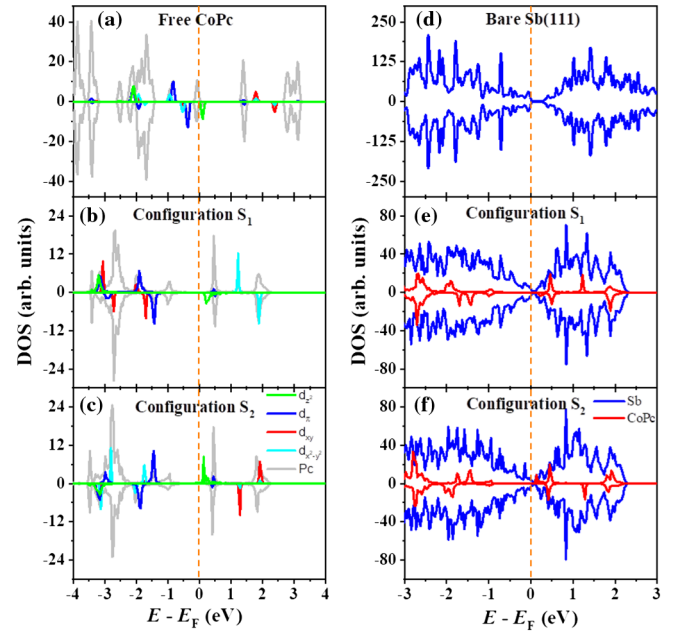


FIG. 2. (a)–(c) Spin-polarized partial density of states of Co and Pc in the free CoPc,  $S_1$ , and  $S_2$  configurations, respectively. The gray, blue, green, red, and cyan curves represent the DOSs of Pc,  $d_x$ ,  $d_{z^2}$ ,  $d_{xy}$ , and  $d_{x^2-y^2}$ , respectively. (d)–(f) Partial density of states of bare Sb(111) and CoPc/Sb(111) composites. The blue and red curves represent the DOSs of Sb and CoPc, respectively.

that the conduction electrons of the Sb(111) around  $E_F$  behave like a perfect “glue” in fine tuning the hybridization strength, such that the molecular spin is preserved due to insignificant charge transfer and yet still effectively coupled to the itinerant electrons to ensure multiple spin-flip scatterings. Our calculations indeed show that the magnetic moments are  $0.962$  ( $S_1$ ) and  $0.943 \mu_B$  ( $S_2$ ), only slightly less than that of the free CoPc ( $0.998 \mu_B$ ). The calculated average distances between the Co ion and the Sb surface are about  $3.37$  ( $S_1$ ) and  $3.31 \text{ \AA}$  ( $S_2$ ). In contrast, previous calculations have shown that the distances of CoPc on various metal substrates in stable configurations are in the range of  $(2.5\text{--}3.0) \text{ \AA}$  [22,23,26,44,45]. Obviously, the Co-Sb distances are larger than that of CoPc on other metal substrates, especially those highly metallic ones. Moreover, our selective test calculations show that the magnetic moment of CoPc is quenched rapidly as the Co-Sb distance decreases (see Fig. S5 in SM [27]). On the basis of these calculations, we conclude that the distance between Co and substrate as well as the interfacial hybridization strengths are mainly controlled by the DOS of the host substrate around  $E_F$ , which is crucial to preserve the molecular spin and drive the CoPc-substrate composites into the Kondo regime.

At a finer level, our calculated spin density maps [Figs. 3(a)–3(d)] of the two configurations show clear spin spreading from the central Co to the pyrrole rings, as also observed in the STM measurements of the Kondo

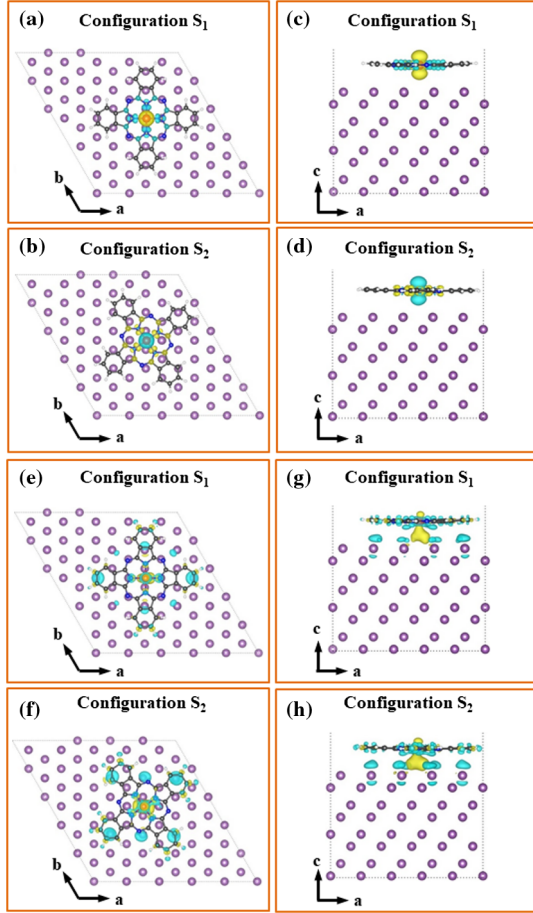


FIG. 3. (a)–(d) Top and side views of the spin distributions for configurations  $S_1$  and  $S_2$ . The spin-up and spin-down contributions are denoted in yellow and cyan, respectively. The isovalue for the spin density is  $0.0006 \text{ e}/\text{\AA}^3$ . (e)–(h) Top and side views of differential electronic density maps for configurations  $S_1$  and  $S_2$ . The yellow and cyan colors represent increase and decrease in the electron density, respectively. The isovalue of the electron density is  $0.0004 \text{ e}/\text{\AA}^3$ .

resonance. In addition, the spin of the ligand is antiparallel to the Co spin, resulting in a minor decrease in the molecular magnetic moment. Nevertheless, the Kondo

resonance in the CoPc-Sb(111) system is not suppressed by the presence of the apparent intramolecular antiferromagnetic coupling.

Our calculated differential electronic density maps of the CoPc-Sb(111) complexes are shown in Figs. 3(e)–3(h). For a given configuration, there exists obvious charge transfer from the surface to the molecule, resulting in the spin-active pyrrole ring due to charge redistribution of the Co ion and ligand. Through Bader charge analysis, we find that  $\sim 0.19$  ( $S_1$ ) and  $0.22e$  ( $S_2$ ) are transferred from the Sb(111) substrate to the CoPc molecules [46]. Moreover, the results also show that the  $3d$  orbital occupations ( $S_1$ : 7.31 and  $S_2$ : 7.34) are similar to that of the free CoPc (7.26), indicating that the molecule has a  $3d^7$  Co(II) center with spin  $1/2$ . Again, we attribute the robust spin of CoPc to the weak interfacial hybridization on the semimetallic Sb(111).

Going beyond isolated admolecules, Fig. 4(a) contrasts the measured Kondo temperature taken from an isolated molecule, a molecular dimer ( $S_1 - S_2$ ), a trimer ( $S_2 - S_1 - S_2$ ), and a much larger island, showing a clear increase in  $T_K$  with the assembly size for the smaller assemblies [see Figs. S6(a) and S6(b) in SM [27]]. We have fitted the  $dI/dV$  spectra (see Fig. S1 in SM [27]) of CoPc in the molecular islands (5 K), yielding  $\Gamma_{\text{fit}} = 31.2 \pm 1.9 \text{ meV}$ . After subtracting the contribution of the modulation signal, we acquire the average values of the physical parameters  $\Gamma = 30.9 \pm 1.9 \text{ meV}$  and  $T_K = 253.6 \pm 16 \text{ K}$ . Figure 4(b) plots the half-width  $\Gamma$  as a function of the temperature from  $T = 5 \text{ K}$  up to  $T = 130 \text{ K}$ , displaying a good fit to the expected formula  $\Gamma = \sqrt{(\pi k_B T)^2 + 2(k_B T_K)^2}$  [[32], see Figs. S6(c) in SM [27]]. We also note that the width of the resonance peak of CoPc in the molecular island is slightly broader than that of an isolated admolecule. According to previous reports, the contributions from magnetic dipolar and direct exchange couplings can be negligible due to the large intermolecular distance (1.56 nm) in the island [35,47]. The observed broadening in the Kondo resonance width may originate from the possible presence of the antiferromagnetic RKKY interaction in the many-body Kondo system [47–49].

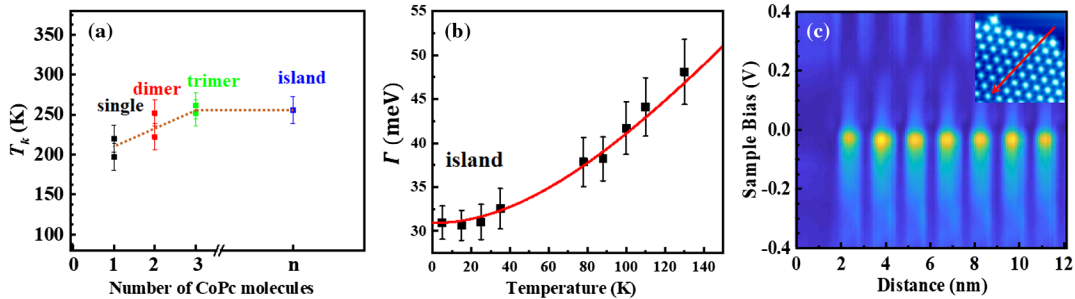


FIG. 4. (a) Kondo temperature as a function of the number of the CoPc assembly size. (b) The half resonance width ( $\Gamma$ ) against measured temperature: the black squares with error bars show the experimental data. (c) Site-dependent  $dI/dV$  spectra of the molecular island acquired along the line with an alternating molecular arrangement of  $S_1$  and  $S_2$  configurations, marked by the red arrow in the upper-right inset.

Figure 4(c) displays the site-dependent  $dI/dV$  spectra along the red arrow shown in the inset, in which the Kondo resonance exhibits good consistency and spatial recognition in a well-ordered molecular island. Given these observations, each CoPc in the molecular island can be exploited as an information storage bit, which may find far-reaching technological applications. More specifically, for the CoPc/Sb(111) system considered here, above the Kondo temperature, the two spin states are well defined, and can be exploited as the information bits “0” and “1”. In the Kondo regime, the two molecular spin states are no longer well defined because of their entanglement with the spins of the itinerant electrons; nevertheless, proper chemical stimulus approaches can still be devised to reversibly switch on or off the Kondo state, thereby restoring their ability to serve as the information bits [50,51]. It is worth noting that here the  $S = 1/2$  states of CoPc/Sb(111) can be exploited as natural binary storage units. In contrast, when MnPc is adsorbed on some good metals such as Ag (001) and Pb(111), its  $S = 3/2$  spin usually preserves or decreases to  $S = 1$  upon accepting one electron from the substrate [20,52,53], and the corresponding quadruplet or triplet states are inherently disadvantageous in defining the bits.

In summary, we discovered pronounced Kondo resonance of CoPc adsorbed on the semimetallic Sb(111) substrate. Our STM/STS results showed that the spin of a CoPc molecule can endure the adsorption on the substrate, inducing complex spin polarization inside the molecule where the pyrrole ring becomes spin active as well. Our DFT calculations further revealed that the optimal density of states of Sb(111) around  $E_F$  plays a crucial role in the preservation of the intrinsic magnetic moment of CoPc while still ensuring sufficiently effective multiple spin-flip scatterings of the conduction electrons of the semimetallic substrate. Moreover, our STS measurements revealed that each of the CoPc molecules in a molecular island exhibits good consistency and spatial recognition of the Kondo resonance, rendering the systems immense potential for applications in ultrahigh-density memory devices. The delicate interfacial physics elucidated in the present study is expected to be also broadly applicable to other related systems combining different magnetic molecules and substrates, including semimetallic substrates with strong spin-orbital coupling, magnetic Weyl semimetallic substrates, and half metals. Such systems may serve as ideal platforms for exploring exotic quantum many-body correlations, spintronic phenomena, and novel topological states of matter, potentially further enriching into unconventional Kondo physics and non-Fermi liquid behavior [54–57].

We acknowledge funding from National Key Research and Development Program of China (Grants No. 2018YFB0407600, No. 2017YFA0303500), National Natural Science Foundation of China (Grants No. 11634011,

No. 11974323, No. 12074099), Strategic Priority Research Program of Chinese Academy of Sciences (Grant No. XDB30000000), the Plan for Leading Talent of Fundamental Research of the Central China in 2020, and Intelligence Introduction Plan of Henan Province in 2021 (CXJD2021008), Anhui Initiative in Quantum Information Technologies (Grant No. AHY170000), Natural Science Foundation for Young Scientists of Henan Province (No. 202300410060), and Key Research Project of Henan Provincial Higher Education (No. 20A140005).

\*These authors contributed equally to this work.

†zhangzy@ustc.edu.cn

‡wzfzhang@henu.edu.cn

- [1] S. Sanvito, *Chem. Soc. Rev.* **40**, 3336 (2011).
- [2] L. Bogani and W. Wernsdorfer, *Nat. Mater.* **7**, 179 (2008).
- [3] E. Moreno-Pineda and W. Wernsdorfer, *Nat. Rev. Phys.* **3**, 645 (2021).
- [4] A. R. Rocha, Víctor M. García-suárez, Steve W. Bailey, Colin J. Lambert, Jaime Ferrer, and Stefano Sanvito, *Nat. Mater.* **4**, 335 (2005).
- [5] G. Czap, Peter J. Wagner, Feng Xue, Lei Gu, Jie Li, Jiang Yao, Ruqian Wu, and W. Ho, *Science* **364**, 670 (2019).
- [6] L. Gu and R. Wu, *Phys. Rev. Lett.* **125**, 117203 (2020).
- [7] A. Zhao *et al.*, *Science* **309**, 1542 (2005).
- [8] U. G. E. Perera, H. J. Kulik, V. Iancu, L. G. G. V. Dias da Silva, S. E. Ulloa, N. Marzari, and S.-W. Hla, *Phys. Rev. Lett.* **105**, 106601 (2010).
- [9] J. Kügel, P.-J. Hsu, M. Böhme, K. Schneider, J. Senkpiel, D. Serrate, M. Bode, and N. Lorente, *Phys. Rev. Lett.* **121**, 226402 (2018).
- [10] S. Javald *et al.*, *Phys. Rev. Lett.* **105**, 077201 (2010).
- [11] L. Farinacci, G. Ahmadi, M. Ruby, G. Reecht, B. W. Heinrich, C. Czekelius, F. von Oppen, and K. J. Franke, *Phys. Rev. Lett.* **125**, 256805 (2020).
- [12] C. Rubio-Verdú, J. Zaldívar, R. Žitko, and J. I. Pascual, *Phys. Rev. Lett.* **126**, 017001 (2021).
- [13] X. Li *et al.*, *Nat. Commun.* **11**, 2566 (2020).
- [14] K. V. Raman *et al.*, *Nature (London) Phys. Sci.* **493**, 509 (2013).
- [15] M. Mannini *et al.*, *Nature (London) Phys. Sci.* **468**, 417 (2010).
- [16] E. Minamitani, N. Tsukahara, D. Matsunaka, Y. Kim, N. Takagi, and M. Kawai, *Phys. Rev. Lett.* **109**, 086602 (2012).
- [17] J. Brede, N. Atodiresei, S. Kuck, P. Lazic, V. Caciuc, Y. Morikawa, G. Hoffmann, S. Blugel, and R. Wiesendanger, *Phys. Rev. Lett.* **105**, 047204 (2010).
- [18] X. Chen, Y. S. Fu, S. H. Ji, T. Zhang, P. Cheng, X. C. Ma, X. L. Zou, W. H. Duan, J. F. Jia, and Q. K. Xue, *Phys. Rev. Lett.* **101**, 197208 (2008).
- [19] L. Gao *et al.*, *Phys. Rev. Lett.* **99**, 106402 (2007).
- [20] E. Minamitani, Y.-S. Fu, Q.-K. Xue, Y. Kim, and S. Watanabe, *Phys. Rev. B* **92**, 075144 (2015).
- [21] A. Mugarza, Cornelius Krull, Roberto Robles, Sebastian Stepanow, Gustavo Ceballos, and Pietro Gambardella, *Nat. Commun.* **2**, 490 (2011).

- [22] J. D. Baran, J. A. Larsson, R. A. J. Woolley, Y. Cong, P. J. Moriarty, A. A. Cafolla, K. Schulte, and V. R. Dhanak, *Phys. Rev. B* **81**, 075413 (2010).
- [23] B. W. Heinrich, Cristian Iacovita, Thomas Brumme, Deung-Jang Choi, Laurent Limot, Mircea V. Rastei, Werner A. Hofer, Jens Kortus, and Jean-Pierre Bucher, *J. Phys. Chem. Lett.* **1**, 1517 (2010).
- [24] S. Stepanow, P. S. Miedema, A. Mugarza, G. Ceballos, P. Moras, J. C. Cezar, C. Carbone, F. M. F. de Groot, and P. Gambardella, *Phys. Rev. B* **83**, 220401(R) (2011).
- [25] F. Schulz, Mari Ijäs, Robert Drost, Sampsa K. Hämäläinen, Ari Harju, Ari P. Seitsonen, and Peter Liljeroth, *Nat. Phys.* **11**, 229 (2015).
- [26] X. Chen and M. Alouani, *Phys. Rev. B* **82**, 094443 (2010).
- [27] See Supplemental Material at <http://link.aps.org/supplemental/10.1103/PhysRevLett.129.026802> for a description of the experimental details and calculated methods, as well as additional experimental data and discussions, which includes Refs. [28–34].
- [28] K. Nagaoka, T. Jamneala, M. Grobis, and M. F. Crommie, *Phys. Rev. Lett.* **88**, 077205 (2002).
- [29] G. Kresse and J. Hafner, *Phys. Rev. B* **47**, 558(R) (1993).
- [30] G. Kresse and J. Furthmüller, *Phys. Rev. B* **54**, 11169 (1996).
- [31] J. P. Perdew, K. Burke, and M. Ernzerhof, *Phys. Rev. Lett.* **77**, 3865 (1996).
- [32] S. L. Dudarev, G. A. Botton, S. Y. Savrasov, C. J. Humphreys, and A. P. Sutton, *Phys. Rev. B* **57**, 1505 (1998).
- [33] Y. Wang, X. Li, and J. Yang, *Phys. Chem. Chem. Phys.* **21**, 5424 (2019).
- [34] S. Grimme, S. Ehrlich, and L. Goerigk, *J. Comput. Chem.* **32**, 1456 (2011).
- [35] L. She, Yinghui Yu, Ping Wu, Yun Zhang, Zhihui Qin, Min Huang, and Gengyu Cao, *J. Chem. Phys.* **136**, 144707 (2012).
- [36] A. Zhao, Zhenpeng Hu, Bing Wang, Xudong Xiao, Jinlong Yang, and J. G. Hou, *J. Chem. Phys.* **128**, 234705 (2008).
- [37] Y. Yu, Limin She, Huixia Fu, Min Huang, Hui Li, Sheng Meng, and Gengyu Cao, *ACS Nano* **8**, 11576 (2014).
- [38] U. Fano, *Phys. Rev.* **124**, 1866 (1961).
- [39] V. Madhavan, W. Chen, T. Jamneala, M. F. Crommie, and N. S. Wingreen, *Science* **280**, 567 (1998).
- [40] A. C. Hewson, *The Kondo Problem to Heavy Fermions* (Cambridge University Press, Cambridge, England, 1993).
- [41] Y. Wang, Xiao Zheng, Bin Li, and Jinlong Yang, *J. Chem. Phys.* **141**, 084713 (2014).
- [42] A. F. Otte, M. Ternes, S. Loth, C. P. Lutz, C. F. Hirjibehedin, and A. J. Heinrich, *Phys. Rev. Lett.* **103**, 107203 (2009).
- [43] A. F. Otte, Markus Ternes, Kirsten von Bergmann, Sebastian Loth, Harald Brune, Christopher P. Lutz, Cyrus F. Hirjibehedin, and Andreas J. Heinrich, *Nat. Phys.* **4**, 847 (2008).
- [44] Z. Hu, Bin Li, Aidi Zhao, Jinlong Yang, and J. G. Hou, *J. Phys. Chem. C* **112**, 13650 (2008).
- [45] A. Mugarza, R. Robles, C. Krull, R. Korytár, N. Lorente, and P. Gambardella, *Phys. Rev. B* **85**, 155437 (2012).
- [46] R. Bader, *Atoms in Molecules: A Quantum Theory* (Oxford University Press, New York, 1994).
- [47] N. Tsukahara, S. Shiraki, S. Itou, N. Ohta, N. Takagi, and M. Kawai, *Phys. Rev. Lett.* **106**, 187201 (2011).
- [48] J. Figgins and D. K. Morr, *Phys. Rev. Lett.* **104**, 187202 (2010).
- [49] P. Wahl, P. Simon, L. Diekhöner, V. S. Stepanyuk, P. Bruno, M. A. Schneider, and K. Kern, *Phys. Rev. Lett.* **98**, 056601 (2007).
- [50] C. Wäckerlin, Dorota Chylarecka, Armin Kleibert, Kathrin Müller, Cristian Iacovita, Frithjof Nolting, Thomas A. Jung, and Nirmalya Ballav, *Nat. Commun.* **1**, 61 (2010).
- [51] H. Kim, Yun Hee Chang, Soon-Hyeong Lee, Yong-Hyun Kim, and Se-Jong Kahng, *ACS Nano* **7**, 9312 (2013).
- [52] J. Kügel, Michael Karolak, Jacob Senkpiel, Pin-Jui Hsu, Giorgio Sangiovanni, and Matthias Bode, *Nano Lett.* **14**, 3895 (2014).
- [53] Y.-S. Fu *et al.*, *Phys. Rev. Lett.* **99**, 256601 (2007).
- [54] D. F. Liu *et al.*, *Science* **365**, 1282 (2019).
- [55] N. Morali, Rajib Batabyal, Pranab Kumar Nag, Enke Liu, Qiunan Xu, Yan Sun, Binghai Yan, Claudia Felser, Nurit Avraham, and Haim Beidenkopf, *Science* **365**, 1286 (2019).
- [56] D. Khadka *et al.*, *Sci. Adv.* **6**, eabc1977 (2020).
- [57] A. Principi, G. Vignale, and E. Rossi, *Phys. Rev. B* **92**, 041107(R) (2015).